Assessment of Different Methods for Drag Penalty Predictions in Rough-Wall Boundary Layers

Medjnoun, T.; Aguiar Ferreira, Manuel; Reinartz, R.; Nugroho, B.; Monty, J.; Hutchins, N.; Ganapathisubramani, B.

DOI
10.1007/978-3-031-55924-2_14

Publication date
2024

Document Version
Final published version

Published in
Progress in Turbulence 10

Citation (APA)
Medjnoun, T., Aguiar Ferreira, M., Reinartz, R., Nugroho, B., Monty, J., Hutchins, N., & Ganapathisubramani, B. (2024). Assessment of Different Methods for Drag Penalty Predictions in Rough-Wall Boundary Layers. In R. Örlü, R. Örlü, A. Talamelli, J. Peinke, & M. Oberlack (Eds.), *Progress in Turbulence 10: Proceedings of the iTi Conference on Turbulence 2023* (pp. 101-106). (Springer Proceedings in Physics; Vol. 404 SPPHY). Springer. https://doi.org/10.1007/978-3-031-55924-2_14

Assessment of Different Methods for Drag Penalty Predictions in Rough-Wall Boundary Layers

T. Medjnoun, M. A. Ferreira, R. Reinartz, B. Nugroho, J. Monty, N. Hutchins, and B. Ganapathisubramani

Abstract Accurate predictions of the drag penalty in rough-wall flows require careful characterisation of surface roughness to determine the equivalent sand-grain roughness height (k_s). The procedure involves measuring wall-shear stress (τ_w) using direct or indirect methods and analyzing velocity profiles. However, indirect methods often rely on assumptions whose validity cannot always be guaranteed. In this paper (partly based on the study [1]), wind tunnel measurements on a realistic rough surface scanned from a fouled ship hull are carried out to evaluate drag penalty predictions. Current data enabled the evaluation of k_s and associated wake parameters using several methods, which were then used for full-scale drag penalty predictions at high Reynolds numbers, with results showing the drag penalty could vary by nearly 15% among methods, highlighting the importance of exercising caution when employing such methods.

T. Medjnoun (✉) · B. Ganapathisubramani
Department of Aeronautics and Astronautics, University of Southampton, Burgess Road, Southampton, Hampshire SO17 1BJ, UK
e-mail: t.medjnoun@soton.ac.uk

M. A. Ferreira
Department of Process and Energy, Delft University of Technology, Delft, Netherlands

R. Reinartz
Department of Applied Physics, Eindhoven University of Technology, Eindhoven, Netherlands

B. Nugroho · J. Monty · N. Hutchins
Department of Mechanical Engineering, University of Melbourne, Grattan Street, Parkville, VIC 3010, Australia

R. Örlü et al. (eds.), *Progress in Turbulence X*, Springer Proceedings in Physics 404,
https://doi.org/10.1007/978-3-031-55924-2_14

1 Roughness Characterisation

The skin-friction coefficient for a zero-pressure gradient turbulent boundary layer can be expressed as,

$$\sqrt{\frac{2}{C_f}} = \frac{1}{\kappa}\ln(\delta^+) + B - \Delta U^+ + 2\frac{\Pi}{\kappa}, \tag{1}$$

with the superscript "+" denoting quantities non-dimensionalised by the friction velocity U_τ and kinematic viscosity ν. Assuming the universality of the Von-Kármán (κ and B) constants. Equation 1 can be rearranged to determine an expression for the roughness function:

$$\Delta U^+ = \overbrace{\sqrt{\frac{2}{C_f^S}} - \sqrt{\frac{2}{C_f^R}}}^{\mathrm{I}} + \overbrace{\frac{1}{\kappa}\ln\left(\frac{\delta^{+R}}{\delta^{+S}}\right)}^{\mathrm{II}} + 2\overbrace{\frac{(\Pi^R - \Pi^S)}{\kappa}}^{\mathrm{III}}, \tag{2}$$

with the superscripts S and R identifying quantities measured over smooth and rough wall flow conditions, respectively, $\delta^+ \equiv Re_\tau$ being the frictional Reynolds number while Π represents the wake strength parameter. Equation 2 denotes three main contributions in the roughness function; changes in (I) frictional drag, (II) frictional Reynolds numbers, and (III) the wake strength parameter. The function governing the wake in the outer flow is assumed to be universal (i.e. universal form), however, the wake strength (i.e. the amplitude of the function) can be different between surfaces. If $\Pi^R = \Pi^S$, then there is universal outer-layer similarity, and ΔU^+ can be determined by substituting the two different values of δ^+ in (2) on top of determining the term I. If also δ^{+R} and δ^{+S} are matched in the presence of universal outer-layer similarity, then ΔU^+ reduces to the difference in the frictional drag, and can be obtained from direct wall-shear stress measurements, without velocity information,

$$\Delta U^+ \equiv \Delta U^+_{DB} = \sqrt{\frac{2}{C_f^S}} - \sqrt{\frac{2}{C_f^R}} \tag{3}$$

When velocity and drag information are both available, ΔU^+ can be determined from the log-layer of the inner-scaled velocity profile. This is done by essentially subtracting the log-law from the measured inner-scaled velocity profile such that:

$$\Psi = U^+ - \left(\frac{1}{\kappa}\ln(\mathrm{y}^+ - \mathrm{d}^+) + \mathrm{B} - \Delta\mathrm{U}^+\right), \tag{4}$$

with d^+ being the zero-plane displacement, considered to be the height at which the mean drag acts. ΔU^+ (together with d^+) is subsequently determined by examining the optimum fit solution that returns the best plateau that occurs within the overlap region. The equivalent sand-grain roughness height k_s can then be determined by exposing the rough surface to different freestream speeds to obtain the variation of ΔU^+ as a function of k_s^+, using the expression:

$$\Delta U^+ \text{ or } \Delta U^+_{DB} = \frac{1}{\kappa}\ln(k_s^+) - C \tag{5}$$

where, C is an additive constant, determined empirically to be equal to 3.5. Once $\Delta U^+/k_s$ are known, the wake strength parameter can be deduced through the modified-log function Ψ, which quantifies the maximum departure from the logarithmic behaviour; $\Pi = \kappa/2 \times \max(\Psi)$.

When drag cannot be directly measured, indirect methods must be employed. In this study, the first indirect method is the comprehensive shear-stress (CSS) method proposed by [2], which follows an iterative error minimisation procedure to determine the friction velocity U_τ using integral momentum equations - total shear stress balance together with the law-of-the-wall. The second method assumes the validity of the outer-layer similarity (OLS) hypothesis implying that both mean and turbulence intensity profiles are similar between the smooth- and rough-wall flows [3]. These different methods are summarised in Table 1.

2 Experimental Methods

Measurements are performed in an open-circuit suction-type wind tunnel at the University of Southampton (as shown in the schematics of Fig. 1). The turbulent boundary layer grows over a flat surface covered with biofouled roughness, with each tile consisting of some tubeworm and 8 barnacles. The barnacles are spaced 0.23δ mm and 0.46δ mm in both x-wise and z-wise horizontal directions, while the maximum roughness height is 6% of the boundary layer thickness δ. To determine the aerodynamic roughness lengthscale, wall-shear stress is directly measured using an in-house floating-element drag balance [4]. The balance is subjected to a series of nine free stream speeds (U_∞) ranging from 9 up to 27 ms^{-1}, with a total of five repetitions per velocity. Pre- and post-calibrations were conducted for each configuration without notable discrepancies. To examine the flow and its homogeneity, velocity fields are obtained from both planar and stereo particle image velocimetry (PIV) at a

Table 1 Methods used for the current biofouled rough-wall flow case study

Method	Wall-shear stress	Flow
Direct	Drag balance	PIV
Equation 3	Drag balance	Assumed
CSS	Log-law+TSS	PIV
OLS	Outer-layer similarity	PIV

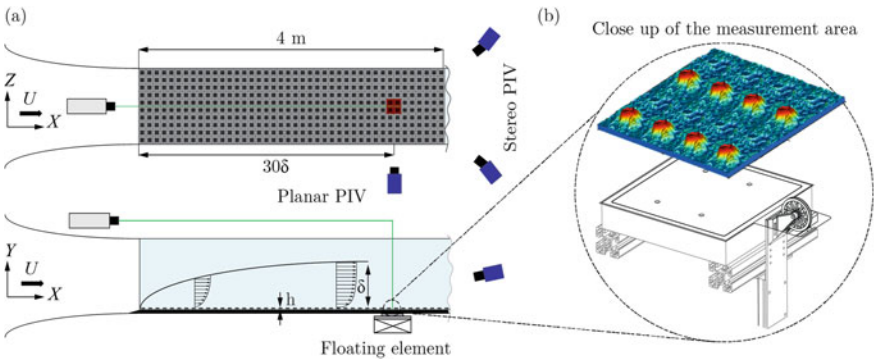

Fig. 1 **a** Schematics of the experimental setup of the planar-and stereo-PIV and **b** a close-up of the floating-element drag balance with the surface topography of a single repeating unit

similar location to that of the drag measurements (equivalent to 30δ downstream the inlet). All planar and stereoscopic PIV measurements are performed in the (x, y)- and (y, z)-planes, respectively, at five free stream speeds ranging from 10 up to 25 ms^{-1}.

3 Results: Lab-Scale

Results from direct drag measurements are shown in Fig. 2a and show that the skin-friction coefficient reaches a constant value, indicating the fully rough regime using the direct method shown by the invariance of C_f as a function of Re_x. However, estimates of the skin-friction coefficient from the OLS method, compared with the direct drag measurements underestimate C_f by close to 10% at the highest Reynolds number, as opposed to 6% when using the CSS method. The reason for this under-estimation is primarily due to a lack of collapse in both the mean and turbulence profiles between the rough and smooth surfaces (not shown for brevity). However, it is worth noting that for both indirect methods, C_f converges weakly towards those values, as the Reynolds number increases, albeit at different rates.

Now that the friction velocity is determined, the roughness function $\Delta U^+(k_s)$ is subsequently deduced by examining the Ψ profiles. Figure 2b shows the results from the different methods and reveals that (3) overestimates $\Delta U^+(k_s)$, while the CSS and OLS methods underpredict $\Delta U^+(k_s)$ as expected. The latter is expected and is a result of the lower estimated friction velocity, however, the former stems from the assumption of outer-layer similarity ($\Pi^R = \Pi^S$), in (3). This can be further explained by combining (2), (3) and (5), which results in the following expression:

$$\Pi^R = \Pi^S + \frac{1}{2}\ln\left(\frac{k_s}{k_{s\,DB}}\right) \tag{6}$$

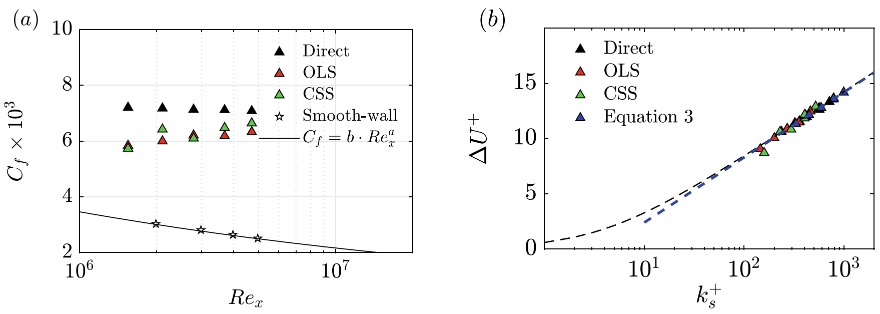

Fig. 2 **a** Variation of the skin-friction coefficient estimated using different methods for Config 1, with the smooth-wall data from [5], and the black solid line representing Schlichting's power-law. **b** Variation of the roughness function estimated the direct and indirect methods, with the solid black line representing the fully rough asymptote

Table 2 Comparison of the aerodynamic parameters results from the direct and indirect methods

Direct	OLS	CSS	Equation 3
$(k_s/\delta - \Pi^R)$	$(k_s/\delta - \Pi^S)$	$(k_s/\delta - \Pi^R)$	$(k_s/\delta - \Pi^S)$
(7.53% – 0.38)	(5.14% – 0.48)	(5.66% – 0.45)	(10.5% – 0.55)

Equation 6 shows that if $\Pi^R = \Pi^S$, then $k_s = k_{sDB}$. However, in the present study, $\Pi^R < \Pi^S$ (due to lack of collapse in the mean and turbulence profiles between smooth- and rough-wall flows), then $k_s < k_{sDB}$, which in turn means ΔU^+ measured will be smaller than ΔU^+_{DB} determined from (3). As also expected, both OLS and CSS methods underestimate the roughness functions. Results from using the different methods are collated in Table 2.

4 Results: Full-Scale Predictions

After determining the aerodynamic roughness parameters, a prediction of the spatially-averaged frictional drag C_F at high Reynolds numbers Re_x (with fixed U_∞ and ν but increasing x) can be made for each pair of (k_s, Π) results. The procedure proposed by [6] is employed, and it consists of an integral boundary layer evolution method based on numerical integration of the skin friction over a given length of the developing flow, assuming a velocity profile composed of a logarithmic and wake region (see [6] for more details).

Results of the full-scale prediction method are depicted in Fig. 3 and show that accurate prediction of skin friction remains possible using (k_s, Π) determined with Eq. 3, provided direct drag measurements at laboratory-scale data are available. Equation 3 results in prediction within 1% to those made by the direct measurements. However, when indirect drag estimates are used, C_F predictions at high Reynolds

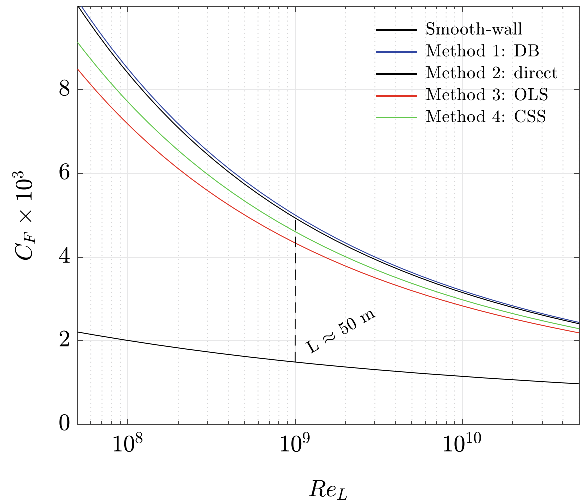

Fig. 3 Prediction of the averaged frictional drag C_F as a function of fetch Reynolds number Re_L at a unit Reynolds number $U_\infty/\nu \approx 2 \times 10^7$ with $U_\infty \approx 18$ ms^{-1} and $\nu \approx 9 \times 10^{-7}$ m^2 s^{-1}

numbers are systematically underestimated. At a Reynolds number of $Re_x \approx 10^9$ (equivalent to a Reynolds number of a 50 m long vessel at full-speed), assuming outer-layer similarity underestimated the frictional drag by over 12% while the comprehensive shear stress method resulted in approximately 6% difference, highlighting the importance of exercising caution when employing such methods. However, these differences tend to decrease as the Reynolds number increases, since most of the drag contributions stem from the changes in the log layer rather than changes in outer-layer wake.

References

1. T. Medjnoun, M.A. Ferreira, R. Reinartz, B. Nugroho, J. Monty, N. Hutchins, B. Ganapathisubramani, Assessment of aerodynamic roughness parameters of turbulent boundary layers over barnacle-covered surfaces. Exp. Fluids **64**(11), 169 (2023)
2. K.M. Womack, C. Meneveau, M.P. Schultz, Comprehensive shear stress analysis of turbulent boundary layer profiles. J. Fluid Mech. (2019)
3. A.A. Townsend, *The Structure of Turbulent Shear Flow*, 2nd edn. (Cambridge University Press, 1976)
4. M.A. Ferreira, E. Rodriguez-Lopez, B. Ganapathisubramani, An alternative floating element design for skin-friction measurement of turbulent wall flows. Exp. Fluids **59**, 155 (2018)
5. T. Medjnoun, C. Vanderwel, B. Ganapathisubramani, Characteristics of turbulent boundary layers over smooth surfaces with spanwise heterogeneities. J. Fluid Mech. **838**, 516–543 (2018)
6. J.P. Monty, E. Dogan, R. Hanson, A.J. Scardino, B. Ganapathisubramani, N. Hutchins, An assessment of the ship drag penalty arising from light calcareous tubeworm fouling. Biofouling **32**, 451–464 (2016)